

## Improving the Near-Field Transmission Efficiency of Nano-Optical Transducers by Tailoring the Near-Field Sample

Kursat Sendur<sup>1</sup> and William Challener<sup>2</sup>

<sup>1</sup>Sabanci University, Istanbul, 34956, Turkey.

<sup>2</sup>Seagate Technology, Pittsburgh, PA 15222, USA.

### ABSTRACT

Despite research efforts to find a better nano-optical transducer for light localization and high transmission efficiency for existing and emerging plasmonic applications, there has not been much consideration on improving the near-field optical performance of the system by engineering the near-field sample. In this work, we demonstrate the impact of tailoring the near-field sample by studying an emerging plasmonic application, namely heat-assisted magnetic recording. Basic principles of Maxwell's and heat transfer equations are utilized to obtain a magnetic medium with superior optical and thermal performance compared to a conventional magnetic medium.

### INTRODUCTION

Emerging plasmonic nano-applications, such as heat-assisted magnetic recording (HAMR), require intense optical spots beyond the diffraction limit. Recent advances in near-field optics achieved spatial resolution significantly better than the diffraction limit. The possible ways to achieve intense optical spots with small sizes include apertures on good metallic conductors [1], bow-tie antennas [2], ridge waveguides [3], and apertureless near-field microscopy [4]. However, the power density requirements of emerging plasmonic applications, such as HAMR, are quite challenging for the nano-optical systems listed above. Therefore, further enhancement in power transmission is necessary.

Despite research efforts to find a better transducer for light localization and high transmission efficiency, there is not much consideration on improving the near-field optical performance of the system by engineering the near-field sample. Some emerging plasmonic applications, such as heat assisted magnetic recording, allow tailoring the shape and composition of the near-field sample. As we demonstrate in this work, a near-field sample has a significant impact on the nano-optical system performance when the sample is designed based on the fundamental principles of optical energy transfer and heat flux propagation.

In this work, we demonstrate the impact of tailoring the near-field sample by studying an emerging plasmonic application, namely heat-assisted magnetic recording [5,6]. The near-field sample in a heat-assisted magnetic recording system is the recording medium. In HAMR, the main requirement is that the temperature of the magnetic medium should be increased to the Curie temperature. Typical Curie temperatures of magnetic materials are on the order of several hundred degrees higher than the ambient temperature. Basic principles of Maxwell's and heat transfer equations are utilized to obtain a magnetic medium with superior optical and thermal performance compared to a conventional magnetic medium. The fundamentals of the optical energy coupling at the optical transducer-magnetic medium interface are explained via Maxwell's equations. Various optical and thermal aspects of the impact on the near-field sample are discussed. The optical performance of the tailored recording medium is compared with a

conventional magnetic medium using 3-D finite element method solutions of Maxwell's and the heat transfer equations when a nano-optical transducer is illuminated with a focused beam of light defined by Richards-Wolf vector field equations. Based on the results, a patterned magnetic medium for HAMR is suggested to increase the optical energy transmission from a near-field transducer to the medium.

## NEAR-FIELD TRANSDUCER-SAMPLE INTERACTION

To understand the optical energy transfer mechanism at the interface between a near-field transducer and a sample, the interaction of various electromagnetic field components produced by a transducer with a sample must be considered. In Fig. 1 a schematic illustration of a ridge waveguide transducer, which is placed at the end of an optical lens system, is provided. The optical transducer is placed in the vicinity of a near-field sample, which is the recording magnetic medium for HAMR. The electromagnetic field distributions at this interface have similarities for different transducers due to Maxwell's boundary conditions for good metals. In a previous study, the  $x$ ,  $y$ , and  $z$  components of the electric field were presented in the magnetic medium when it was in the vicinity of a ridge waveguide [7]. Figures 3-5 in that study suggest that the strength of the perpendicular (i.e.  $z$ ) component of the electrical field is comparable to or even larger than the transverse (i.e.  $x$  and  $y$ ) components. Since the transducer acts as an electric dipole, it would be expected to produce significantly stronger transverse component than the perpendicular component. Within the transducer, strong transverse field components are present. Outside the transducer, especially in the space between the transducer and the recording medium, a stronger perpendicular component is present. The presence of a stronger perpendicular component can be best understood by the boundary conditions on good metals. Good metals force the electric field lines to be perpendicular to their surface. Strong perpendicular electric field components are even more prominent for apertureless optical transducers [4]. Sample electric field distributions around transducers can be found in the literature [7-8].

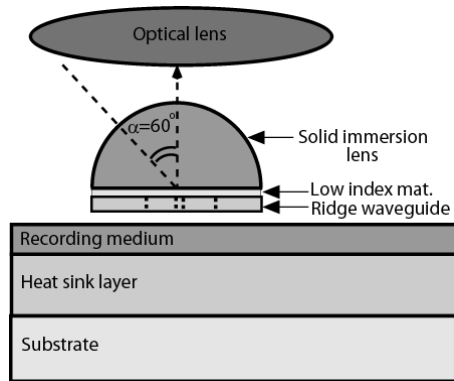


**Figure 1.** A schematic illustration of an optical transducer, which is placed at the end of an optical lens system, is given. The optical transducer is placed in the vicinity of a near-field sample, which is the recording magnetic medium for HAMR.

In light of this discussion, the main concern for practical plasmonic systems is to efficiently couple the strong perpendicular component of the electric field into the sample. Coupling of the electric fields into the recording medium determines the transmission efficiency of the system. The coupling of the electric fields at the interface between the transducer and the

magnetic medium are determined by the boundary conditions. Maxwell's equations state that: (a) the tangential component of the electric field across an interface between two media is continuous,  $\vec{E}_1^t = \vec{E}_2^t$ , (b) the perpendicular component of the electric field intensity across an interface is discontinuous by an amount  $\vec{E}_1^n / \vec{E}_2^n = \varepsilon_2 / \varepsilon_1$ , where  $\varepsilon_1$  and  $\varepsilon_2$  are the permittivities of each material.

For different applications, the permittivity of the sample exhibits a large variation. In HAMR, the permittivity of magnetic materials at optical frequencies is significantly larger in magnitude than the permittivity of materials that fill the interface. The perpendicular component of the electric field in the magnetic medium is very low for the conventional magnetic medium. This results in low coupling efficiency for the perpendicular component of the electric field into a conventional magnetic medium. Since a strong perpendicular electric field is present at the interface between the transducer and magnetic medium, the discontinuity of the perpendicular component reduces the optical energy coupling from the transducer into the magnetic medium.

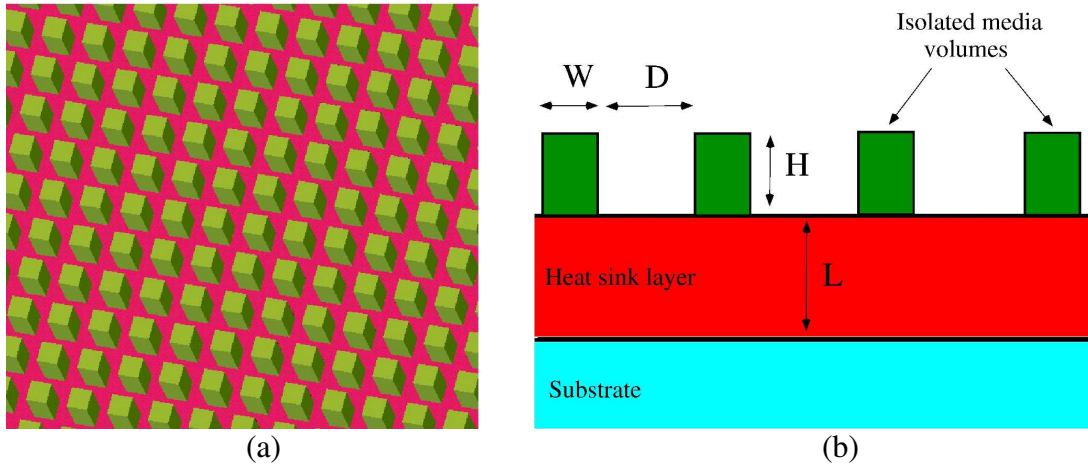


**Figure 2.** (a) An oblique view of the patterned magnetic medium with optically and thermally isolated magnetic particles placed over a heat sink layer, (b) Patterned magnetic medium with optically and thermally isolated magnetic particles placed over a heat sink layer. The geometric dimensions of the particle size and separation as well as the thicknesses of the magnetic and heat sink layers are shown.

## RESULTS

The sample in the near-field systems can be designed so that the coupling of the perpendicular electric field component into the sample can be significantly improved. For example, in HAMR the magnetic medium, shown in Fig. 2, has a number of electromagnetic and thermal advantages over the conventional recording medium, including better electromagnetic field coupling and reduced thermal spread in the lateral direction. The designed medium, shown in Fig. 2, uses isolated magnetic volumes to increase both the light coupling and the thermal response. Isolated metallic volumes are made of magnetic material such as a CoPt alloy. Dielectric volumes are placed between these magnetic grains to isolate them both optically and thermally. The medium utilizes a highly conducting metallic heat-sink underlayer which quickly removes the heat from the medium. Fast heat removal is necessary for high recording data rates.

The improvement of localized heating in the magnetic medium shown in Fig. 2 is demonstrated using numerical simulations. Finite element method (FEM) 3-D electromagnetic and thermal modeling software is used. The finite element method (FEM) is a well-known numerical algorithm for the solution of Maxwell's equations [9]. In this study, a frequency-domain based FEM [10] is used for the solution of Maxwell's equations. Tetrahedral elements are used to discretize the computational domain, which allows modeling of arbitrarily shaped three-dimensional geometries. Over the tetrahedral elements, the edge basis functions and second-order interpolation functions are used to expand the functions. Adaptive mesh refinement is employed to improve the coarse solution regions with high field intensities and large field gradients. For thermal modeling, an FEM [10] based solution is used as well. FEM is a well-known and efficient computational technique, widely used for the solution of the heat transfer problems. In this study, we used commercially available FEM based thermal modeling software, which employs a time-domain-based FEM formulation for the solution of the heat transfer equation. FEM utilizes a Galerkin formulation, which minimizes the mean error over the computational volume. A combination of hexahedral, pentahedral, and tetrahedral elements are used to discretize the computational volume. Second-order interpolation functions are used to expand the unknown functions.

To illustrate the effect of the patterned medium shown in Fig. 2, we obtained 3-D finite element method solutions of Maxwell's and the heat transfer equations. The specifications of the numerical simulation are as follows. The transducer was illuminated with an optical power source of 100 mW. The recording medium model in this work is composed of uniformly-distributed same-size magnetic particles, which are equally separated from each other. The magnetic particles have side lengths of 5 nm. The separation between the particles is 5 nm and the height is 10 nm. The optical source produces about 30 nm spot size, which mainly illuminates the central 9 particles under the transducer. A heat sink layer with a 200 nm thickness is placed under the magnetic particles. The operating wavelength of the optical source is 700 nm. The thermal and optical properties of the magnetic layer and the heat sink layer are listed in Table 1. Figures 3 (a) and (b) illustrate the temperature distribution through a contour on the top surface of the recording medium. As shown in Figs. 3 (a) and (b), a higher temperature and a tighter localization are obtained by using a recording medium as shown in Fig. 2, instead of a conventional recording medium. Such high temperatures and small spots are essential for a practical HAMR system. Another potential area of interest for patterned near-field sample, which is described in this work, is optical data storage. Other examples of engineering near-field samples are discussed in the literature [11-12].

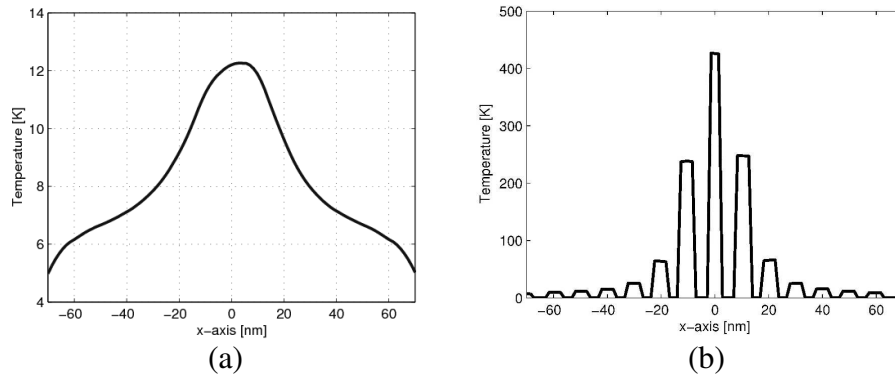


**Figure 3.** Temperature distribution in the (a) continuous recording medium and (b) patterned recording medium for a magnetic particle size of 5 nm and the duty cycle is 50%.

**Table 1.** Thermal and optical properties of the magnetic layer and the heat sink layer.

Layer	Density [W/m <sup>3</sup> ]	Specific Heat [J/(kg K)]	Thermal Conductivity [W/(m K)]	Refractive Index [unitless]
Magnetic layer	8862	421	99.2	0.16 + i 3.95
Heat sink layer	19300	129	317	2.30 + i 4.43

The higher temperature and tighter localization shown in Fig. 3 (b) are primarily achieved by better optical coupling of electromagnetic waves into the patterned medium shown in Fig. 2 compared to conventional recording medium. In the case of a conventional recording medium, the electric field lines are perpendicular to the medium, as shown in Fig. 4 (a). However, in the case of patterned media, the electric field lines are perpendicular on the top surfaces and tangential on the side surfaces of the medium, as shown in Fig. 4 (b). The perpendicular component of the electric field intensity across an interface is discontinuous, but the tangential component of the electric field across an interface between two media is continuous. Due to this continuity, the tangential components of the field couple better to the medium. Better coupling of electromagnetic fields results in higher optical power absorption in the recording medium shown in Fig. 2.

In addition to better optical coupling, the patterned medium shown in Fig. 2 provides more favorable thermal conditions compared to a conventional recording medium. In the patterned medium shown in Fig. 2, the heat loss via lateral thermal conduction is greatly reduced because of the thermally insulating material between the magnetic particles. A decrease in lateral thermal conduction reduces the heat transfer to adjacent bits, and therefore, increases the temperature in the magnetic particle. The insulating material between the magnetic volumes also helps to prevent the thermal spread in the lateral direction, therefore, tighter thermal localization is achieved in Fig. 3 (b).

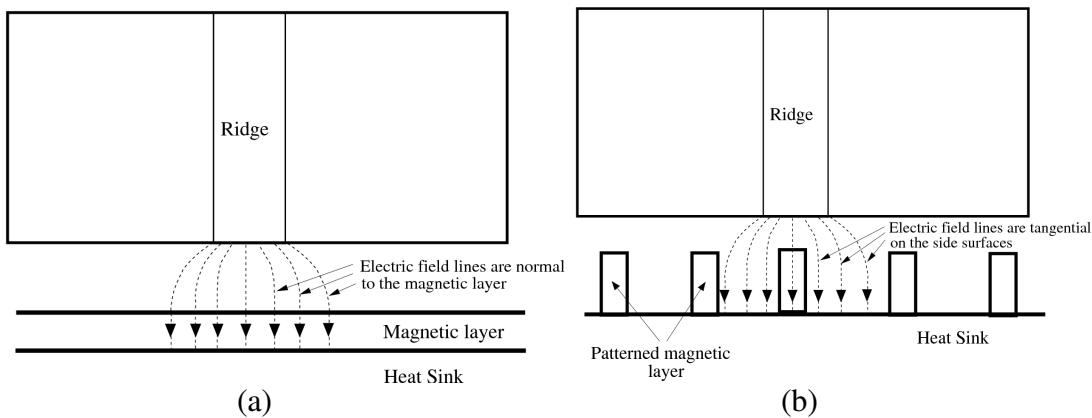


**Figure 4.** (a) Continuous recording medium is illustrated in the vicinity of a ridge waveguide. The electric field lines are normal to the continuous recording medium. (b) The electric field lines are both normal (at the top surfaces) and tangential (on the side surfaces) to the patterned media.

To achieve higher transmission efficiencies, and therefore, higher temperatures in the magnetic particles around the optical transducer, the sparsity  $S$  of the magnetic medium and the width of the magnetic particles should be reduced and the height  $H$  of the particles should be

increased. This will make the media volumes more isolated and the electric field will better couple to the media due to the increase in the tangential component. Also the volumes become more thermally isolated, which will increase the temperatures. However, as previously mentioned, inappropriate selection of these parameters may result in a magnetically unstable medium. Therefore, these parameters should be optimized considering magnetic stability and the optical transducer performance.

The experimental conditions on the manufacturing of a patterned medium will also have an impact on the power transmission into the magnetic medium. The shape of the isolated media pattern volumes is an important factor determining the optical absorption in the recording medium. Particles with long and sharp side walls provide better optical absorption in the medium. Experimental imperfections, such as rough edges or undesired edge steepness, will reduce power transmission to the magnetic medium.

## CONCLUSIONS

In summary, optical energy coupling at the interface between an optical transducer and near-field sample was explained via the boundary conditions of Maxwell's equations. Based on this description, the basic principles are applied to tailor the design of the near-field sample in HAMR. A patterned magnetic medium was suggested to increase the optical energy transmission from the near-field transducer to the medium. Results suggest that optically and thermally isolated magnetic particles can be used to increase the light coupling and temperature response in HAMR.

## REFERENCES

1. F. J. G. de Abajo, *Opt. Express* 10, 1475 (2002).
2. R. D. Grober, R. J. Schoelkopf, and D. E. Prober, *Appl. Phys. Lett.* 70, 1354 (1997).
3. X. Shi and L. Hesselink, *Jpn. J. Appl. Phys.* 41, 1632 (2001).
4. A. Hartschuh, E. J. Sánchez, X. S. Xie, L. Novotny, *Phys. Rev. Lett.* 90, 095503 (2003).
5. T. McDaniel, W. Challener, and K. Sendur, *IEEE Trans. Mag.* 39, 1972 (2003).
6. R. Rottmayer et al., *IEEE Trans. Mag.* 42, 2417 (2006).
7. K. Sendur, W. Challener, and C. Peng, *J. Appl. Phys.* 96, 2743 (2004).
8. W. Challener et al., *Jpn. J. Appl. Phys.* 45, 6632-6642 (2006).
9. J. M. Jin, *The finite element method in electromagnetics* (John Wiley & Sons, New York, NY, 2000).
10. All the FEM calculations in this report are performed with software from Ansoft Inc. and Ansys Inc.
11. F. Hao et al., *Phys. Rev. B* 76, 245417 (2007).
12. D. W. Brandl et al., *Chem. Phys.* 123, 024701 (2005).